Proceedings of Coastal and Ocean Engineering in Korea (2002)
Vol. 13, pp. 1-13

Review: Development of Numerical Wave Flume CADMAS-SURF (SUper Roller Flume for Computer Aided Design of MAritime Structure)

Koji Fujima[1] (Research Group on Application of Numerical Wave Flume to Maritime Structure Design[2])

1. INTRODUCTION

1.1 Maritime-structure Design and Numerical Simulation

For design of maritime structure, it is necessary to evaluate the effect and stability of the structure against wave action. Laboratory model experiments and their empirical formulas are mainly used to estimate those at present, although empirical formulas have a problem of accuracy and hydraulic experiments of cost and duration. In addition, performance-based design, which may be popularized as a new design concept in the near future, requires much more information than that obtained by empirical formulas and laboratory tests. Thus, numerical simulation may become more important hereafter for structure design.

Numerical simulation was introduced into coastal engineering in the latter of 1950s. In Japan, the first numerical work was, perhaps, the simulation of storm surge of the 1959 Typhoon of Ise-bay. Thereafter, linear wave theory such as mild slope equation was applied to predict the wave transformation. At present, nonlinear effect can be considered sufficiently in the practical simulation. However, many of those are horizontally two-dimensional model, hence it is not easy to express wave splash and turbulent complicated flows caused by wave breaking. Thus, it is difficult to evaluate the effect and stability of maritime structure against wave action directly by numerical simulation.

However, recently, the CFD (Computational Fluid Dynamics) becomes popular even in coastal, harbor and ocean engineering. In the CFD, the governing equations based on adequate modeling are solved numerically to clarify the characteristics of fluid motion. Using the technique of CFD, it becomes possible to reproduce the complicated flow around structure. Because the CFD technology keeps improving considerably, we can expect that the direct application of numerical simulation to maritime-structure design will be realized in the near future.

In Europe, and also in Japan, many investigations are conducted on this theme in recent years (e.g., Troch, 1997). In these works, the VOF (Volume Of Fluid) method (Hirt and Nichols, 1981) is widely used as the practical manner to handle the multiple free-surface boundaries and to reproduce the complicated phenomenon with strong nonlinearity.

To investigate the application of numerical simulation to maritime structure design intensively, a research group was organized, and the group developed the code of numerical wave flume available for various problems. In this paper, outline and prospects of this code is presented. This numerical code is based on the VOF method, and is applicable to not only wave transformation but also interaction of wave, current, structure and foundation. Namely, this numerical flume is replaceable with the laboratory flume, and applicable to the practical works of maritime- structure design against wave action.

1.2 Research Group

The 'Research group on application of numerical wave flume to maritime structure design' was established in 1998. The group consisted of about 30 researchers of university, government and non-government institute of Japan; Professor Isobe, University of Tokyo, acted as the chair and CDIT (Coastal Development Institute of Technology) as the office. The activities of the group are summarized as follows:

(1) Development of numerical code

A two-dimensional numerical wave flume was developed, where a personal computer is placed as the general platform of computation (Isobe et al., 1999). The

[1] Dept. of Civil and Environmental Eng., National Defense Academy, Yokosuka 239-8686, JAPAN
[2] Office: Coastal Development Institute of Technology, Sumitomo-Hanzomon Bldg., Tokyo 102-0092

code was written in FORTRAN and arranged in order so as to make improving and updating the code easy. The basic performance, e.g. performance of wave-generator boundary, non-reflecting boundary and so on, were checked sufficiently. This code is called 'CADMAS-SURF' (SUper Roller Flume for Computer Aided Design of MAritime Structure). CADMAS-SURF was developed to evaluate the effect and stability of structure, thus it can consider the effect of wave breaking and complicated free surface accurately enough.

(2) Application to maritime structure design

The developed numerical wave flume was applied to the design of various maritime structures. Through these attempts, some problems were clarified; then the numerical flume was improved and updated. In addition, know-how of the use of the code was accumulated (CDIT, 2001).

1.3 Open-source Policy

The research group expects that the worldwide engineers use the numerical wave flume CADMAS-SURF and it promotes the application of numerical simulation to structure design. Thus, the group decided to distribute the source code. Many researchers maybe challenge to improve the program, thus the source code is simply written in FORTRAN considering the future improvement and extension. The research group had ended once, however, CDIT can collect and disseminate the information required for improving the program. The load module of CADMAS-SURF and the detailed explanation on it is attached in the technical report of the research group in a form of CD-ROM. CDIT is now constructing the web site to distribute the source code (http://www.cdit.or.jp).

2. SPECIFICATIONS OF CADMAS-SURF

2.1 Outline

There are several methods to analyze the transient flow with multiple free-surface boundaries, e.g. the MAC method (Harlow and Welch, 1965), the ALE method (Hirt et al., 1972), the C-CUP method (Yabe and Wang, 1991), the Level Set method (Sussman et al., 1994) and so on. Among them, the VOF method is relatively practical, and applicable to the complicated phenomenon. The numerical wave flume is necessary to analyze the multiple free-surface boundaries and apply to the various conditions. Thus, CADMAS-SURF adopts the VOF method to analyze the free surface and the SMAC (Simplified Marker And Cell) method (Amsden and Harlow, 1970) to analyze the velocity-pressure field. Specifications of CADMAS-SURF are summarized in Table 1-3.

Table 1. Specifications on physical model of CADMAS-SURF

Item	Functions
Object of analysis	• Two-dimensional incompressible flow with multiple free-surface boundaries
Governing equation	• Navier-Stokes (Reynolds) equation and continuity equation for two-dimensional incompressible fluid based on porous body model
Coordinate system	• Cartesian coordinate
Free surface model	• VOF (Volume Of Fluid) method
Turbulence model	• High Reynolds number $k-\varepsilon$ two equation turbulence model
Wave generation model	• Wave-generator boundary • Wave generation source (The following wave-generation functions are available for each wave-generation model)
Target function for wave generation	• Fifth-order Stokes wave • Third-order cnoidal wave • Stream function method B • Piston-type wave generator • Flap-type wave generator • Generation of arbitrary wave with matrix data
Open (non-reflecting) boundary	• Sommerfeld's radiation condition • Energy dissipation zone
Transport of scalar variable	• Applicable to an arbitrary advective diffusion equation of scalar variable (Notice: it is necessary to edit a user-subroutine in the program)
Other boundary conditions	• Possible to set an obstacle at arbitrary location • Possible to set a boundary condition on arbitrary position of obstacle face • Possible to select a boundary condition using input data (slip, non-slip, constant velocity, logarithmic law (smooth and rough surface), and outflow)

2.2 Basic Model

To analyze a wave field in coastal region, it is necessary to consider the bottom topography and complicated configuration of structure such as permeable caisson. Thus, Navier-Stokes (Reynolds) equations and the continuity equation for two-dimensional incompressible fluid modified by the porous-body method are adopted as governing equations as follows:

Table 2. Specifications on numerical scheme and algorithm of CADMAS-SURF

Item	Functions
Discretization	• Finite difference method with staggered mesh • Shape approximation with porous body model
Time-integration	• Euler method • SMAC (Simplified Marker And Cell) method
Advection term	• Selectable from the following schemes (except for the equation of VOF function) (1) First-order upwind difference scheme (2) Second-order central difference scheme (3) DONOR scheme (hybrid of (1) and (2)) (4) QUICK scheme • Advection term in the equation of VOF function is discretized with donor-acceptor method
Treatment of velocity on surface cell	• Extrapolation (extrapolation from velocities inside the fluid) • Zero-gradient (set the same velocity as on neighbor full-cell)
Determination of free surface direction	• NASA-VOF3D method
Treatment of air bubble and water droplet	• TimerDoor method
Solver of simultaneous linear equation	• MILU-BCGSTAB method
Control of time increment	• Fixed • Automatic

Table 3. Specifications on data-output and visualization of CADMAS-SURF

Item	Functions
Time-series data	• Continuous output of water surface elevation at a specified location • Continuous output of a variable at a specified point
Visualization of spatial distribution of a variable at specific time	• Velocity vector • Isogram of variable • Free surface • Coloring of water region
Support for making animation	• Continuous output of visualization data (bmp form) with a fixed time interval

$$\frac{\partial \gamma_x u}{\partial x}+\frac{\partial \gamma_z w}{\partial z}=S_\rho \tag{1}$$

$$\begin{aligned}\lambda_v\frac{\partial u}{\partial t}&+\frac{\partial \lambda_x uu}{\partial x}+\frac{\partial \lambda_z wu}{\partial z}=-\frac{\gamma_v}{\rho}\frac{\partial p}{\partial x}\\&+\frac{\partial}{\partial x}\left\{\gamma_x \nu_e\left(2\frac{\partial u}{\partial x}\right)\right\}+\frac{\partial}{\partial z}\left\{\gamma_z \nu_e\left(\frac{\partial u}{\partial z}+\frac{\partial w}{\partial x}\right)\right\}\\&-D_x u+S_u-R_x\end{aligned} \tag{2}$$

$$\begin{aligned}\lambda_v\frac{\partial w}{\partial t}&+\frac{\partial \lambda_x uw}{\partial x}+\frac{\partial \lambda_z ww}{\partial z}=-\frac{\gamma_v}{\rho}\frac{\partial p}{\partial z}\\&+\frac{\partial}{\partial x}\left\{\gamma_x \nu_e\left(\frac{\partial w}{\partial x}+\frac{\partial u}{\partial z}\right)\right\}+\frac{\partial}{\partial z}\left\{\gamma_z \nu_e\left(2\frac{\partial w}{\partial z}\right)\right\}\\&-D_z w+S_w-R_z-\gamma_v g\end{aligned} \tag{3}$$

where, t is the time, x and z the horizontal and vertical coordinates, u and w the velocity components, ρ the density, p the pressure, ν_e the summation of kinetic viscosity ν and eddy viscosity ν_t, g the gravitational acceleration, γ_v the porosity, and γ_x and γ_z the parameters for cell-surface permeability. In addition, D_x and D_z are the parameters used for energy dissipation zone, and S_ρ, S_u and S_w are for wave generation source, which will be denoted later.

The coefficients λ_v, λ_x and λ_z are denoted as follows, where the second terms in R.H.S. (C_M :inertia coefficient) expresses the inertia force affected by structure.

$$\left.\begin{aligned}\lambda_v&=\gamma_v+(1-\gamma_v)C_M\\\lambda_x&=\gamma_x+(1-\gamma_x)C_M\\\lambda_z&=\gamma_z+(1-\gamma_z)C_M\end{aligned}\right\} \tag{4}$$

The resistance force from the porous body is modeled as follows:

$$R_x=\frac{1}{2}\frac{C_D}{\Delta x}(1-\gamma_x)u\sqrt{u^2+w^2} \tag{5}$$

$$R_z=\frac{1}{2}\frac{C_D}{\Delta z}(1-\gamma_z)w\sqrt{u^2+w^2} \tag{6}$$

where, C_D is the drag coefficient, Δx and Δz the grid size in horizontal and vertical direction, respectively.

The VOF method is adopted to analyze the free surface boundary. In the VOF method, the advective equation of the VOF function F, which implies the ratio of fluid volume to cell volume, are solved; and the cell flag,

which distinguishes 'full-cell', 'surface-cell' and 'empty-cell', is computed successively. The advective equation of the VOF function based on the porous body model is expressed as follows:

$$\gamma_v \frac{\partial F}{\partial t} + \frac{\partial \gamma_x u F}{\partial x} + \frac{\partial \gamma_z w F}{\partial z} = S_F \tag{7}$$

where S_F is the source term required for wave-generation source method. Note that the VOF function has a different meaning from the void ratio, and is introduced to express the free surface sharply. Thus, donor-acceptor method is used to compute the above equation to keep the clear boundary.

As a turbulence model, $k-\varepsilon$ (two-equation) model for high Reynolds number is adopted, which is widely used for the practical purposes. The basic equations are the advective diffusion equations for the turbulent kinetic energy k and the dissipation rate of the turbulent kinetic energy ε as follows:

$$\gamma_v \frac{\partial k}{\partial t} + \frac{\partial \gamma_x u k}{\partial x} + \frac{\partial \gamma_z w k}{\partial z} = \frac{\partial}{\partial x}\left\{\gamma_x \nu_k \left(\frac{\partial k}{\partial x}\right)\right\} + \frac{\partial}{\partial z}\left\{\gamma_z \nu_k \left(\frac{\partial k}{\partial z}\right)\right\} + \gamma_v G_s - \gamma_v \varepsilon \tag{8}$$

$$\gamma_v \frac{\partial \varepsilon}{\partial t} + \frac{\partial \gamma_x u \varepsilon}{\partial x} + \frac{\partial \gamma_z w \varepsilon}{\partial z} = \frac{\partial}{\partial x}\left\{\gamma_x \nu_\varepsilon \left(\frac{\partial \varepsilon}{\partial x}\right)\right\} + \frac{\partial}{\partial z}\left\{\gamma_z \nu_\varepsilon \left(\frac{\partial \varepsilon}{\partial z}\right)\right\} + \gamma_v C_1 \frac{\varepsilon}{k} G_s - \gamma_v C_2 \frac{\varepsilon^2}{k} \tag{9}$$

$$G_s = \nu_t \left\{2\left(\frac{\partial u}{\partial x}\right)^2 + 2\left(\frac{\partial w}{\partial z}\right)^2 + \left(\frac{\partial w}{\partial x} + \frac{\partial u}{\partial z}\right)^2\right\} \tag{10}$$

The eddy viscosity and diffusion coefficients of the above equations are expressed as follows:

$$\nu_t = \frac{C_\mu k^2}{\varepsilon} \tag{11}$$

$$\nu_k = \nu + \frac{\nu_t}{\sigma_k} \tag{12}$$

$$\nu_\varepsilon = \nu + \frac{\nu_t}{\sigma_\varepsilon} \tag{13}$$

where, the general values are adopted for the empirical coefficients in the above equations; namely, $C_\mu = 0.09$, $\sigma_k = 1.00$, $\sigma_\varepsilon = 1.30$, $C_1 = 1.44$, $C_2 = 1.92$ (Launder and Spalding, 1974).

2.3 Wave-Generation Model

As shown in Table 1, CADMAS-SURF adopts the wave-generator boundary and the wave- generation source for wave-generation model. For both models, six kinds of wave generation functions are available, five are for regular waves and one is for irregular waves.

In the wave-generation source method, it is not necessary to set the velocities and water elevation directly as the boundary conditions; hence the reflected wave from structure or sloping beach can be transmitted the source location. Thus, non-reflecting wave generation is realized by using the wave-generation source method with the energy dissipation zone and/or the radiation boundary condition, which will be stated later. The source terms should be set at the source location $x = x_s$, the center of a specified cell, in the wave generation source model. The source terms are expressed as follows:

$$S_\rho = q(z,t) \tag{14}$$

$$S_u = uq(z,t) \tag{15}$$

$$S_w = wq(z,t) + \frac{\nu}{3}\frac{\partial q(z,t)}{\partial z} \tag{16}$$

$$S_F = Fq(z,t) \tag{17}$$

Here, $q(z,t)$ is denoted by the following equation, in which Δx_s is the grid size at $x = x_s$, $U(z,t)$ the velocity for wave generation modified to prevent the increase of water quantity in the flume.

$$q(z,t) = 2\frac{U(z,t)}{\Delta x_s} \tag{18}$$

2.4 Non-reflecting Boundary

Both Sommerfeld's radiation condition and the energy dissipation zone are available in CADMAS-SURF to make a non-reflecting boundary.

(1) Sommerfeld's radiation condition

$$\frac{\partial f}{\partial t} + C\frac{\partial f}{\partial x} = 0 \tag{19}$$

Here, f denotes a physical variable such as velocity, C the wave celerity. At present, the small amplitude wave (Airy) theory is used to estimate C. Thus, to apply to nonlinear waves, it should be used together with the following energy dissipation zone.

(2) Energy dissipation zone

The energy dissipation zone damps the reflected wave energy gradually in the region of 1-3 wavelength. Through this manner, a non-reflecting boundary is realized. This method requires the additional computational area, although it has the advantages on the applicability to various wave conditions and the stability of numerical simulation.

In CADMAS-SURF, the damping terms proportional to the velocity are considered in the equations of motion, the coefficients are as follows:

$$D_x = \theta_x \sqrt{\frac{g}{h}} (N+1) \left(\frac{x - x_0}{l} \right)^N \tag{20}$$

$$D_z = \theta_z \sqrt{\frac{g}{h}} (N+1) \left(\frac{x - x_0}{l} \right)^N \tag{21}$$

where, h is the water depth, l and x_0 the length and starting location of the energy dissipation zone, respectively, N the exponent of distribution function, θ_x and θ_z the non-dimensional coefficients.

2.5 Basic Performance of CADMAS-SURF

The research group examined the basic performance of CADMAS-SURF such as wave generation, wave absorbing, wave propagation on horizontal bottom, wave shoaling, and breaking wave height. If the computed results differed from the theoretical or experimental results, the code was improved and updated (CDIT, 2001).

Note that there are some cases where the computed results are affected considerably by the computational grid or the scheme of advection term. Thus, the adequate know-how is required to obtain the accurate results at present. In addition, when a wave breaks, a large fluctuation is found in the computational results wave-by-wave, as in laboratory tests. Thus, a user should record the output data during several wave periods, and ensemble-average the data to compare it with other data. Besides, it is difficult to reproduce the detailed wave profile when it breaks. This should be improved hereafter.

3. APPLICATION OF CADMAS-SURF TO STRUCTURE DESIGN

3.1 Outline

CADMAS-SURF is able to simulate the wave transformation on various conditions, and is applicable to the problem of interaction of wave, current, foundation and structure. Thus, CADMAS-SURF can simulate most experiments conducted by a laboratory wave flume, and is applicable to many coastal-structure designs.

Figure 1 demonstrates the scheme of application of CADMAS-SURF to structure design. Because the wave profile, velocity, acceleration, pressure and so on are obtained by CADMAS-SURF, the wave shoaling, transmitted wave height, wave force and so on are directly evaluated by CADMAS-SURF. The quantity of wave overtopping is also evaluated through the velocity and water surface elevation on breakwater body, and the reflection coefficient is through the wave power passing a control surface. The research group applied to the simulations of wave runup, wave transformation on a reef and submerged breakwater, wave transformation with breaking on an uniform sloping beach, propagation of bore, transmission coefficient and wave force acting on permeable structures (e.g. submerged breakwater, curtain wall, submerged horizontal plate, L-shaped curtain wall, and step-type wave-absorbing breakwater), wave-overtopping quantity and wave force acting on wall-type structures (e.g. upright wall, seawall covered with wave-dissipating blocks, semi-submerged sloping-top caisson breakwater, and wave-absorbing caisson breakwater), and so on (Takahashi and Ikeya, 2000a; Kawasaki et al., 2000; Takahashi et al., 2001 Takahashi and Ikeya, 2000b; Fujii et al., 2000; Nakano et al., 2001; Sanuki et al., 2001; Arikawa et al., 2001; Kotake et al., 2001; CDIT, 2001).

In addition, if a time-history of wave force is obtained, for example, the sliding distance of a caisson can be estimated through its equation of motion. The wave force acting on a pile may be also evaluated from the velocity and acceleration if the drag and inertia coefficients are determined properly. The research group examined judging the stability of armor materials through Isbash equation with the velocity near the mound (Matsumoto and Takahashi, 2001).

On the other hand, it is possible to evaluate the stability of armor materials by solving the other numerical module such as the DEM (Discrete Element Method) simultaneously with CADMAS-SURF. The impulsive wave force due to air bubbles will be computed by simultaneously solving the adequate model such as Bagnold model. The research group tried to extend CADMAS-SURF by linkage with the DEM for analyzing the rubble mound and the FEM (Finite Element Method) for analyzing the foundation (Itoh et al., 2000; Itoh et al., 2001; Fujii et al., 2001; Jang et al., 2000).

In this section, we will show some examples of the application of CADMAS-SURF.

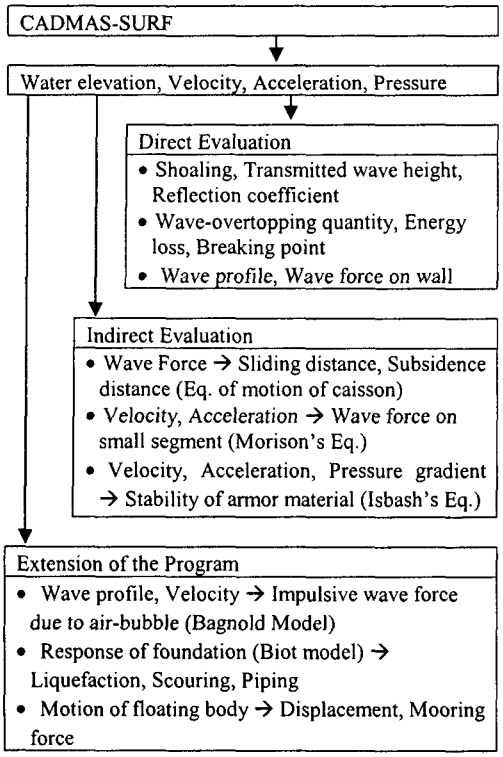

Figure 1. Application of CADMAS-SURF.

3.2 Upright seawall: Wave profile

Firstly, let us show the examination on the reproducibility of breaking wave profile conducted by Arikawa et al. (2001). They compared the numerical results with the results of laboratory experiments on the wave collision with a caisson wall conducted by Takahashi et al. (1983). In the laboratory tests, the wave flume was 160m in length, and the offshore part was the flat floor with water depth of 80cm (about 130m in length), the nearshore part the flat floor with water depth of 40cm, and the middle part the sloping bottom of gradient of 1/10 (4m in length); the caisson wall was set at the location B_1 from the edge of the nearshore horizontal floor. In the computations, the offshore part was simplified as about 20m in length to shorten the computation time.

Figure 2 shows the wave profiles in the case where the vertical wave front just before breaking collides with the wall then the wave pressure shows a sharp peak of Wagner type. Figure 3 shows the profiles in the case where the wave collides with the wall after its breaking then the wave pressure of Bagnold type is observed. The time phases in photos taken in the experiments are not clear, thus the numerical wave profiles cannot be compared directly with the experimental ones. However, in both cases, the numerical simulations reproduce the tendency of variation of wave profile accurately. Arikawa et al. (2001) reported that the simulations provided the accurate results even in the wave pressure observed at the wall.

3.3 Submerged breakwater: Wave pressure

Next, the reproducibility of wave pressure acting on a submerged breakwater with rectangular section is demonstrated (CDIT, 2001). The laboratory experiments were conducted with the model of 1/60 scale. In prototype scale, the offshore part was the flat floor 39.4m in water depth and 280m in length, the middle part was the sloping beach of 1/30 in gradient and 720m in length, and the nearshore part the flat floor 15.4m in water depth and 1000m in length. The submerged breakwater, 10.4m in height and 20m in length, was set near the edge of the nearshore flat floor. The incident waves were the regular waves whose height was H = 4m and period T = 8,10,12,14,16s.

In the numerical simulations, the advection terms were computed by the scheme of DONOR-0.2 (weighted average of the upwind difference with the first order accuracy and the central difference with the second order accuracy, the weight of upwind difference is 0.2 and the weight of central difference 0.8). The grid size in vertical direction was 0.8m, and the grid size in horizontal direction was ranging 1.25m to 2.5m, which was determined by a simple guideline of $L/80$, where L is the wavelength.

Figure 4 (a) and (b) show the wave pressure distributions in the typical cases. The numerical results of CADMAS-SURF (solid line) agree well with the experimental results. On the other hand, the numerical results of the BIEM (Boundary Integral Equation Method) agree with the experimental ones measured at the fore face of breakwater in rushing phase, but not with those measured at the rear face. In addition, in ebbing phase of the case with long wave-period, accuracy at the fore face also becomes worse; hence the BIEM tends to overestimate the total force in ebbing phase. It is concluded that, even for the case of submerged breakwater whose submerged depth of crown is small then nonlinearity is strong, CADMAS-SURF provides accurate results and is superior to the BIEM.

3.4 Seawall covered with wave-dissipating blocks: Wave-overtopping quantity

The conventional diagram and the empirical formula for evaluating the wave-overtopping quantity are convenient for practical works, although they are valid only for the limited conditions. Thus, laboratory model experiments are usually conducted to estimate the overtopping quantity for an actual structure. Here, to examine the applicability of CADMAS-SURF, the laboratory tests on wave overtopping conducted by Sakakiyama and Imai (1996) was reproduced (Nakano et al., 2001).

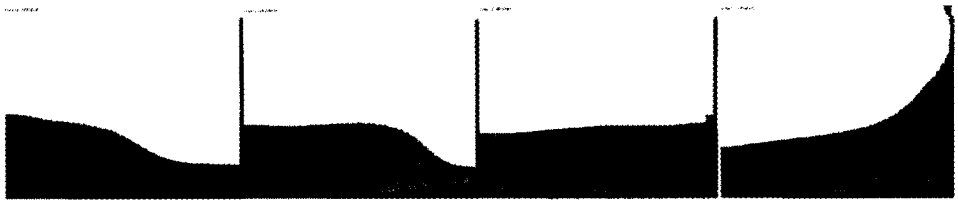

(a) CADMAS-SURF (0.2s intervals)

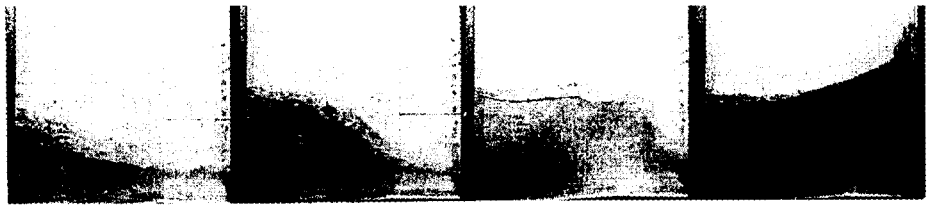

(b) Experimental photographs

Figure 2. Profiles of wave colliding with a vertical wall. ($B_1 = 0.25\text{m}$).

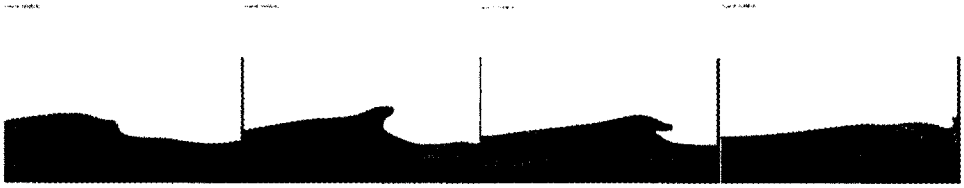

(a) CADMAS-SURF (0.2s intervals)

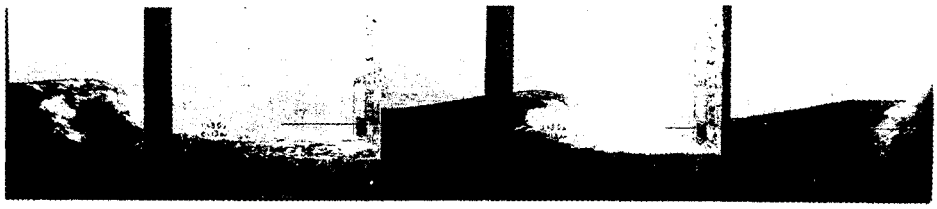

(b) Experimental photographs

Figure 3. Profiles of wave colliding with a vertical wall. ($B_1 = 1.75\text{m}$).

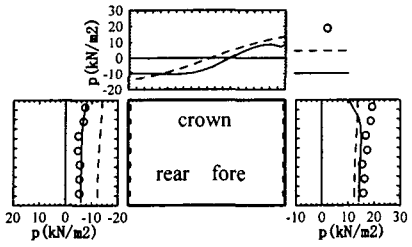

(a) T=8s

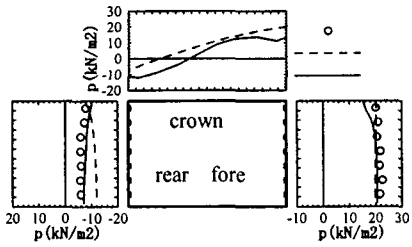

(b) T=12s

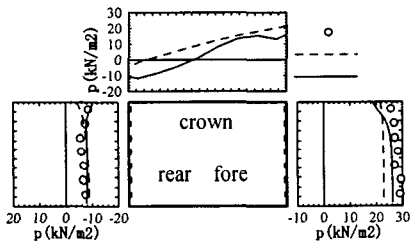

(c) =16s

Figure 4. (a) Distribution of wave pressure in rushing phase.

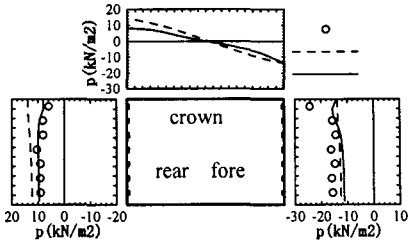

(a) T=8s

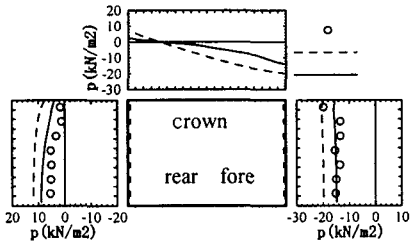

(b) T=12s

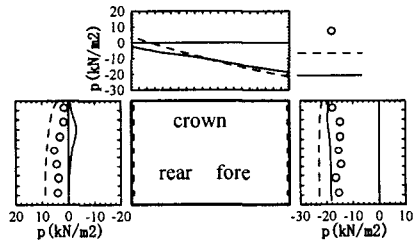

(c) =16s

Figure 4. (b) Distribution of wave pressure in ebbing phase.

The laboratory experiments were conducted with a two-dimensional wave flume 20m in length, 0.3m in width and 0.55m in depth. The water depth was 0.3m. The upright caisson (seawall) model whose crown height was 5cm and width 30cm and the wave-absorbing works were set on the flat bottom. The wave absorbing works was composed of a block having a weight of 60g; the slope was 3/4 and the two blocks set at the crown. The overtopped water was accumulated in a measure, and the overtopping quantity was estimated by averaging the increase of the weight of the measure for one period. Sakakiyama and Imai (1996) carried out 16 cases of experiments, although the results of five cases will be shown here. The standard condition is $H = 10\text{cm}$ and $T = 1.4\text{s}$, and the wave period and wave height are varied from the standard values. In the numerical computations, the horizontal and vertical grid size was 1cm and 0.5cm, respectively, and the scheme of advection term was DONOR-0.1. The porosity of wave absorbing works was set 0.5, inertia coefficient 1.5 and drag coefficient 0.9, following Sakakiyama and Imai (1996).

Figure 5 shows the overtopping situation in the case of $H = 10\text{cm}$ and $T = 1.4\text{s}$, with the time interval of $T/8$. In Figure 5 (a) and (b), interaction of the wave running up the wave-absorbing woks with the flow returning inside the works forms a complicated velocity field. The phase of fluid motion inside the absorbing works is delayed in comparison to the incident wave

motion, and the water elevation inside the absorbing works rises after the wave runup. In (c), the overtopped water flows on the crown. In (d)-(f), the overtopped water keep their motion, but the wave runs down on the absorbing works. These flow situations agree with those observed in the experiments satisfactorily.

Figure 6 shows the comparisons of the averaged quantity of wave overtopping obtained by the experiments and CADMAS-SURF. The left figure compares the results of the cases in which the wave period is fixed 1.4s but the wave height is varied. On the other hand, the wave period is varied in the right figure. For the reference, the results without setting absorbing-works (namely, the case of upright seawall) are shown in the right figure. In both figures, the numerical results agree well with the experimental ones. In the case of $T = 1.0\mathrm{s}$, the numerical simulation slightly underestimates the overtopping quantity, although the numerical value is about 0.87—1.15 times the experimental value. Thus, CADMAS-SURF provides accurate results in comparison to the numerical simulations of Sakakiyama and Imai (1996).

In addition, in the case of $T = 1.0\mathrm{s}$, the overtopping quantity on the wave-absorbing revetment is smaller than that on the upright seawall because of the energy dissipation effect of wave absorbing works; however, in the cases of $T = 1.4, 1.6\mathrm{s}$, the wave-absorbing seawall provides the larger overtopping quantity than the upright seawall, because the effect of wave runup predominates over the effect of energy dissipation in absorbing works. This characteristic is consistent with the experimental facts obtained by Sakakiyama and Imai.

3.5 Rubble mound breakwater: Combination with DEM

Because CADMAS-SURF solves the universal fundamental equations directly, and adopts the VOF method, it can reproduce very complicated phenomenon such as wave breaking and overtopping, which were difficult to be reproduced by the conventional method. Taking this advantage, it is possible to solve the motion of structure simultaneously with the motion of fluid.

In the structure resistive design against wave action, the structure deformation is expected to be within a range in which the effect of structure is kept enough. At present, the structure deformation is generally checked by the laboratory model tests. We can expect that the numerical experiment of CADMAS-SURF is available for complement of the laboratory tests as a convenient and economical tool by combining with a structure analysis.

Ito et al. (2000, 2001) investigated the deformation of rubble mound breakwater, which was modeled to be composed of a sphere with a fixed diameter, by combining with the DEM (Discrete Element Method). Through these examinations, they demonstrated the possibility of extending the application area of CADMAS-SURF.

CADMAS-SURF and the DEM are coupled by the following procedure; (1) the rubble mound is modeled as the porous body, and the fluid motion is analyzed; (2) the fluid force acting on a sphere is computed by the velocity inside the rubble mound; (3) based on the fluid force, gravitational force, buoyancy force, and so on, the motion of a sphere particle is solved by the DEM; (4) the parameters in the porous body method are re-estimated with considering the deformation of structure, and the fluid motion at the next step is analyzed. Repeating this procedure, the fluid motion and structure deformation can be analyzed simultaneously.

Figure 7 shows the results of laboratory model experiment, in which the glass sphere was used as the material of rubble mound breakwater. An air chamber was set in the flume, and a water column of the height of H was generated in the chamber by sucking air. By instant release of the valve, a strong current with wave breaking was generated in the flume. Figure 7 shows the photographs taken in the case of $H = 60\mathrm{cm}$. In the figure, the wave incident from left side propagates to right side, and the time interval of photograph is not constant. The motion of particle is not uniform in the direction of flume width, although the situation of failure of the breakwater can be observed. When the wave plunges, the glass particle at both tops of slope begins to move, and it is transported considerably
when the water surface slope is large. Figure 8 shows the numerical results. The marks (1)-(4) in the figures show the correspondence of time between the experiment and simulation. The simulation reproduces the wave breaking (1), the movement of glass particle at both tops of slope (2), and the situation of failure of the breakwater (3, 4).

In this computation, the fluid force acting on a particle is evaluated by Morison's equation, in which the relative velocity to the particle velocity is used. Besides, the sheltering effect by neighbor particles is considered to evaluate the fluid force. If the sheltering effect is ignored, a particle at the top of left slope (upstream side) is pushed out strongly so that the structure deformation is overestimated. Ideally, the sheltering effect by neighbor particles should be evaluated by the fluid analysis through the porous model. However, to do so, very small grid is required in the computation. At present, it is practical that the sheltering effect is considered at the evaluation of fluid force.

As shown in the present computation, the coupling simulation of CADMAS-SURF and the DEM succeeded to reproduce the deformation of rubble mound breakwater qualitatively. This fact clearly suggests the possibility of the application of the numerical simulation to the performance-based design of structure.

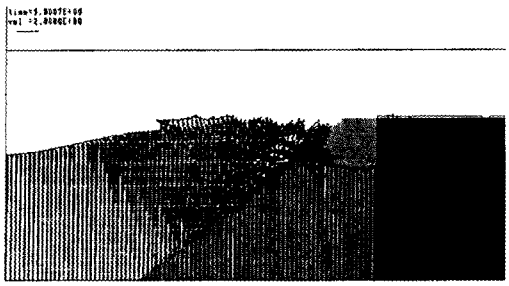

(a) t/T=7.000

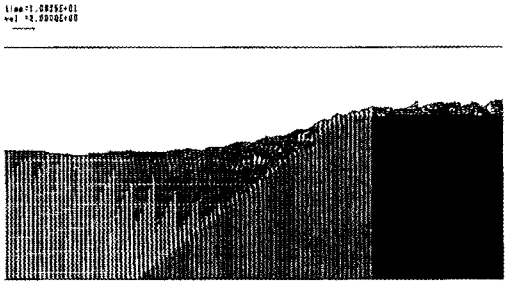

(d) t/T=7.375

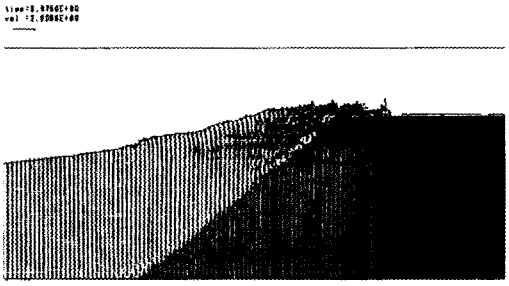

(b) t/T=7.125

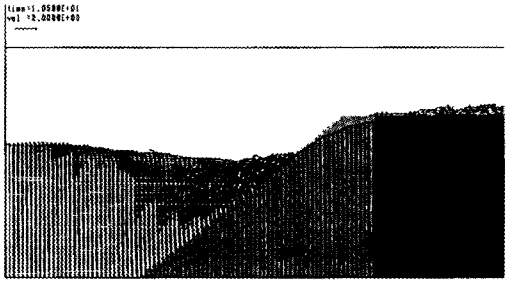

(e) t/T=7.450

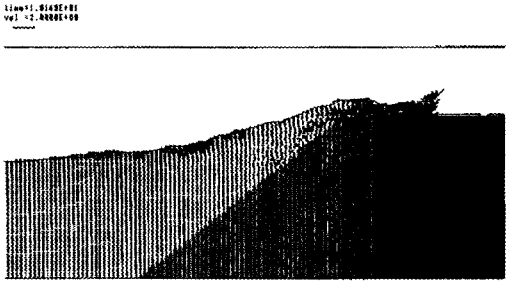

(c) t/T=7.249

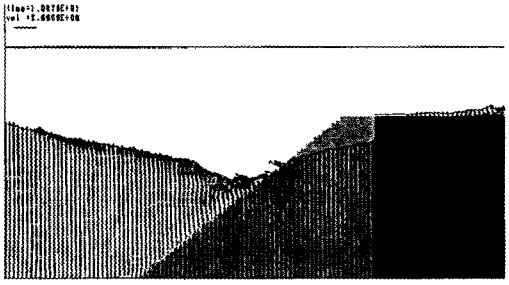

(f) t/T=7.626

Figure 5. Velocity vectors in wave overtopping over wave dissipating revetment. (H=10cm, T=1.4s)

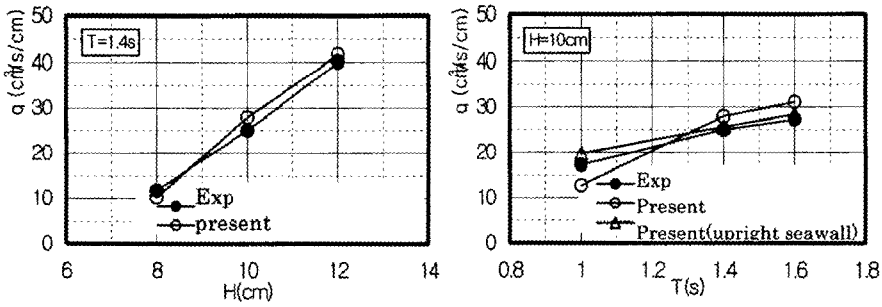

Figure 6. Comparisons of averaged wave-overtopping quantity.

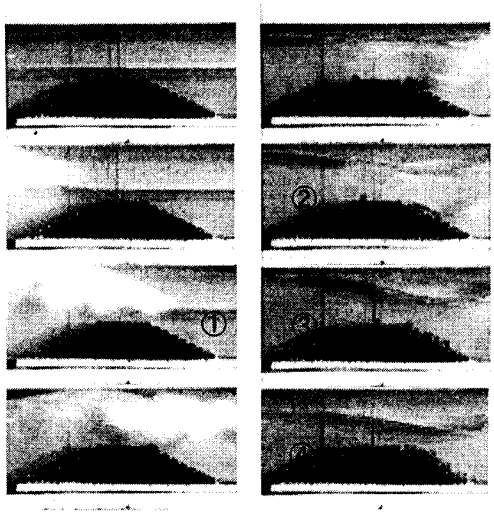

Figure 7. Experimental results on the failure of rubble mound breakwater.

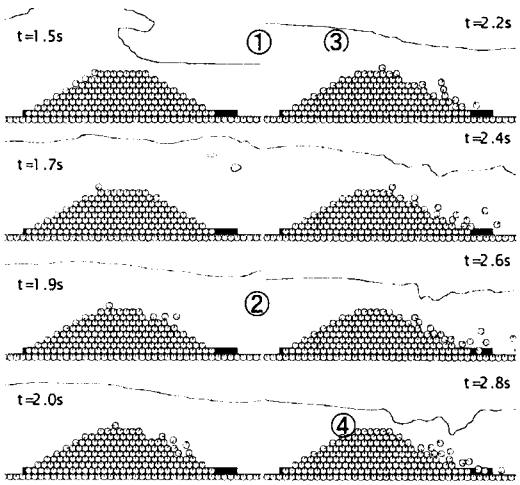

Figure 8. Numerical results on the failure of rubble mound breakwater. (H=60cm)

4. PROSPECTS

4.1 Improvement of the code

Through various applications of CADMAS-SURF, some problems in the present code were pointed out. The major problem was of the computation time. The research group conducted many cases of computations, although there was several cases whose computation time exceeded a few hours. However, a personal computer is improving considerably, thus this drawback will be overcome in the future. In addition, the present code is not tuned-up to shorten the computation time, because the versatility and extensibility are important at the present stage.

On the reproducibility of the phenomena, the present code can provide rather satisfactory results in general. However, some problems on the reproducibility still remain, e.g. wave damping by numerical viscosity, reproducibility of breaking wave profile, and effect of compressed air bubble. These problems of the present code will be improved hereafter by not only the research group but also the other worldwide engineers. If it may be difficult to find a simple solution of these problems, some extension of specification may be required.

More systematic investigation is desirable even for the extension of the program, e.g. linkage with other modules such as the DEM.

Besides, the extension to three-dimensional program is clearly important. In the technical meaning, it may be not so difficult to develop the three dimensional program. In fact, we know that there are a few universal business codes for three-dimensional fluid analysis. At present, a 3D computation may not be practical because of the computation cost. However, a 3D computation will be applied firstly to a relatively simple problem, such as the case where a small pile is set in a 2D wave flume. In addition, Fujima et al. (2001) developed the hybrid model of 2D and 3D computation for tsunami analysis. Similar attempt is interesting also for CADMAS-SURF. Anyway, sooner or later, a 3D computation will be practical in the future. Note that the research group restricted the objects of simulation to two-dimensional phenomenon in the present version of CADMAS-SURF, although the extensibility to 3D was considered in the programming.

4.2 Numerical wave flume and performance-based design

In the 21st century, civil Engineers will be desired to clarify the failure probability, the scale and effect of deformation, and the required maintenance of the structure when they will make a plan. Namely, it will be important to demonstrate the performance of structure in detail, with precision (Takahashi and Shimosako, 2001).

Not only laboratory model experiment but also numerical simulation is necessary to examine the performance of structure against various conditions accurately. A numerical wave flume is an effective tool to conduct a large amount of precise examinations of performance. Besides, numerical simulation facilitates the visualization of phenomenon, thus it is suitable for an account to the residents, which is vital to the future

design.

In the future, the conventional empirical formulas such as Goda's equation or Hudson's equation may be used for the preliminary design of structure, and the detailed examinations on performance-based design for the final *design. In the performance-based design, many* numerical simulations will be carried out so that the effect and stability of the structure should be examined in detail, and the design of the structure such as an optimum section of structure should be determined by the sufficient examinations.

ACKNOWLEDGMENTS

The author would like to appreciate all members of the research group for their cooperation. The group members are listed as follows:

Prof. Masahiko Isobe (University of Tokyo, Chair); Dr. Shigeo Takahashi, Dr. Taro Arikawa (Port and Airport Research Institute); Dr. Jiang; Prof. Xiping Yu (Shanghai Jiao Tong University); Prof. Koji Fujima (National Defense Academy); Dr. Koji Kawasaki (Osaka University); Dr. Tsutomu Sakakiyama (Central research Institute of Electric Power Industry); Dr. Tsuyoshi Ikeya, Dr. Toshihiko Takahashi, Dr. Ryosuke Asakura (Kajima corporation); Dr. Toru Memita, Dr. Noriaki Yagi (Kansai Electric Power Co.); Dr.Tsunehiro Sekimoto, Dr. Takuzo Shimizu, Yoichi Moriya, Ryu Fujita (Penta-Ocean Construction Co.); Dr. Hidehiro Katsui, Dr. Kazunori Itoh (TAISEI Co.); Dr. Akio Nakamura (Chubu Electric Power Co.); Dr. Katsuhiro Satoh, Dr. Akira Matsumoto (TETRA Co.); Dr. Michio Gomyo, Dr. Toshio Aono (TOA Co.); Dr. Toshiya Kyono, Dr. Osamu Nakano (Tokyo Electric Power Co.); Dr. Naoki Fujii (Tokyo Electric Power Service Co.); Dr. Ryuichi Fujiwara, Dr. Yasuo Kotake (Toyo Construction Co.); Dr. Koichi Tsuruya, Dr. Hiroyuki Yamatani, Dr. Sosuke Kitazaawa, Dr. Kozo Wada, Dr. atsuhiro Tadokoro, dr. Hiroshi Oyama, Dr. Yasuhiro Matsushita, Dr. Yutaka Miyawaki (CDIT); Dr. Akio Shimada, Dr. Akihiro Hamano, Dr. Minoru Akiyama, and Dr. Shigenori Oshima (Fuji Research Institute Co.).

REFERENCES

Amsden, A.A. and Harlow, F.H., 1970. A simplified MAC method for incompressible fluid flow calculations,. *J. Computational Phys.*, 6, pp. 322-325.

Arikawa, T., Isobe, M. and Takahashi, S., 2001. Numerical simulation of impulsive breaking wave pressure by VOF method. *Proc. Coastal Eng.*, JSCE, 48, pp. 831-835. (in Japanese)

Coastal Development Institute of Technology, 2001. Investigation and development of numerical wave flume: CADMAS-SURF. CDIT library No.12, CDIT, 296p.

Fujii, N. , Aono, T., Kyono, T. and Nakano, O., 2000. Application of numerical wave flume to evaluation of wave force and overtopping quantity on caisson breakwater. *Proc. Coastal Eng.*, JSCE, 47, pp. 706-710. (in Japanese)

Fujii, N. , Kyono, T., Yasuda, K. and Okuma, Y., 2001. Simulation of sliding of caisson breakwater by DEM. *Proc. Coastal Eng.*, JSCE, 48, pp. 801-805. (in Japanese)

Fujima, K., Masamura, K. and Goto, C., 2001. 2D/3D hybrid model Numerical simulation of submerged breakwater deformation by r tsunami numerical simulation. *Proc. Int. Workshop on Advanced Design of Maritime Structure in 21st Century*, Yokosuka, PHRI, pp. 218-223.

Harlow, F.H. and Welch, J.E., 1965. Numerical calculation of time-dependent viscous incompressible flow of fluid with free surface. *Phys. Fluids*, 8(12), pp. 2182-2189.

Hirt, C.W., Amsden, A. and Cook, J., 1972. An arbitrary Lagrangian-Eulerian computing method for all flow speed. *J. Computational Phys.*, 14, pp. 227-253.

Hirt, C.W. and Nichols, B.D., 1981. Volume of fluid (VOF) method for dynamics of free boundaries. *J. Computational Phys.*, 39, pp. 201-225.

Isobe, M., Hanahara, Y., Yu, X. and Takahashi, S., 2001. A VOF-based numerical model for wave transformation in shallow water. *Proc. Int. Workshop on Advanced Design of Maritime Structure in 21st Century*, Yokosuka, PHRI, pp. 200-204.

Isobe, M., Takahashi, S., Isobe, M., Takahashi, S., Yu, X., Sakakiyama, T., Fujima, K., Kawasaki, K., Jiang, Q., Akiyama, M. and Oyama, H., 1999. Interim report on development of numerical wave flume for maritime structure design. *Proc. Civil Eng. in Ocean*, JSCE, 15, pp. 321-326. (in Japanese)

Isobe, M., Yu, X., Umemura, K. and Takahashi, S., Takahashi, 1999. Investigation ofn development of nuerical wave flume. *Proc. Coastal Eng.*, JSCE, 46, pp. 36-40. (in Japanese)

Itoh, K., Higuchi, Y., Toue, T. and Katsui, H., 2001. Prediction of submerged breakwater deformation with random rubble motions by DEM. *Proc. Coastal Eng.*, JSCE, 48, pp. 806-810. (in Japanese)

Itoh, K., Toue, T. and Katsui, H., 2001. Numerical simulation of failure of particulate structure by DEM and VOF method. *Proc. Coastal Eng.*, JSCE, 47, pp. 746-750. (in Japanese)

Itoh, K., Toue, T. and Katsui, H., 2001. Numerical

simulation of submerged breakwater deformation by DEM. *Proc. Int. Workshop on Advanced Design of Maritime Structure in 21st Century*, Yokosuka, PHRI, pp. 302-309.

Jiang, Q., Takahashi, S. and Isobe, M., 1999. On applicability of numerical wave flume to evaluation of wave force. *Proc. Coastal Eng.*, JSCE, 46, pp. 41-45. (in Japanese)

Jiang, Q., Takahashi, S., Muranishi, Y. and Isobe, M., 2000. Development of VOF-FEM prediction model with interaction of wave, foundation and structure. *Proc. Coastal Eng.*, JSCE, 47, pp. 51-55. (in Japanese)

Kotake, Y., Fujiwara, R., Takahashi, S. and Isobe, M., 2001. Evaluation of reflection performance of perforated caissons by VOF numerical simulations. *Proc. Int. Workshop on Advanced Design of Maritime Structure in 21st Century*, Yokosuka, PHRI, pp. 310-316.

Kotake, Y., Matsumura, A., Fujiwara, R., Takahashi, S. and Isobe, M., 2001. Applicability of VOF method to estimation of reflection coefficient of upright wave-absorbing caisson breakwater. *Proc. Coastal Eng.*, JSCE, 48, pp. 1016-1020. (in Japanese)

Launder, B.E. and Spalding, D.B., 1974. The numerical computation of turbulent flows. Computer Methods in Applied Mechanics and Engineering, 3, pp. 269-289.

Matsumoto, A. and Takahashi, S., 2001. A new design method of armor unit of composite breakwater based on velocity field analysis. *Proc. Coastal Eng.*, JSCE, 48, pp. 911-915. (in Japanese)

Miyata, H., Katsumata, M., Lee, Y.G. and Kajitani, H., 1988. A finite difference simulation model for strongly interacting two-layer flow. *J. Soc. Naval Archit., Japan*, 163, pp. 1-16.

Nakano, O., Kyono, T., Fujii, N. and Sakakiyama, T., 2001. Numerical simulation of wave overtopping and transmitted wave over seawall and breakwater by numerical wave flume. *Proc. Coastal Eng.*, JSCE, 48, pp. 731-735. (in Japanese)

Sakakiyana, T. and Imai, S., 1996. Numerical simulation of wave overtopping on wave absorbing revetment, *Proc. Coastal Eng.*, JSCE, 43, pp. 696-700. (in Japanese)

Sanuki, H., Fujita, R., Sekimoto, T. and Shimizu, T., 2001. Estimation of wave-overtopping quantity by numerical model. *Proc. Coastal Eng.*, JSCE, 48, pp. 736-740. (in Japanese)

Sussman, M., Smereka, P., and Osher, S., 1994. A level set approach for computing solutions to incompressible two-phase flow. *J. Computational Phys.*, 114, pp. 146-159.

Takahashi, S. and Shimosako, K., 2001. Performance design for maritime structures and its application to vertical breakwaters— Caisson sliding and deformation-based reliability design. *Proc. Int. Workshop on Advanced Design of Maritime Structure in 21st Century*, Yokosuka, PHRI, pp. 63-73.

Takahashi, S., Tanimoto, K. and Suzumura, S., 1983. Generation mechanism of impulsive pressure by breaking wave on a vertical wall. *Rep. Port & Harbor Res. Inst.*, PHRI, 22(4), pp. 3-31.

Takahashi, T., Fujima, K., Asakura, R. and Ikeya, T., 2001. An application of numerical wave flume to transformation of bore. *Proc. Civil Eng. in Ocean*, JSCE, 17, pp. 281-286. (in Japanese)

Takahashi, T. and Ikeya, T., 2000. Application of a numerical wave flume to wave transformation on a reef. *Proc. Civil Eng. in Ocean*, JSCE, 16, pp. 69-74. (in Japanese)

Takahashi, T. and Ikeya, T., 2000. Application of a numerical wave flume to step-type wave absorbing breakwaters. *Proc. Annual Conf. JSCE*, JSCE, 55(2), pp. 60-61. (in Japanese)

Troch, P., 1997. VOFbreak2, A numerical model for simulation of wave interaction with rubble mound breakwaters. *Proc. 27th IAHR Congress*, San Francisco, pp. 1366-1371.

Yabe, T. and Wang, P.Y., 1991. Unified numerical procedure for compressible and incompressible fluid. *J. Phys. Soc. Japan*, 60(7), pp. 2105-2108.